The Wnt modulator sFRP2 enhances mesenchymal stem cell engraftment, granulation tissue formation and myocardial repair

Maria P. Alfaro[a], Matthew Pagni[a,b], Alicia Vincent[a,b], James Atkinson[a,b], Michael F. Hill[c], Justin Cates[a], Jeffrey M. Davidson[a,b], Jeffrey Rottman[b,c], Ethan Lee[d], and Pampee P. Young[a,b,c,1]

Departments of [a]Pathology, [c]Internal Medicine, and [d]Cell and Developmental Biology, Vanderbilt University School of Medicine, Nashville, TN 37232; and [b]Department of Veterans Affairs Medical Center, Nashville, TN 37232

Edited by Darwin J. Prockop, Tulane University, New Orleans, LA, and approved October 8, 2008 (received for review April 10, 2008)

Cell-based therapies, using multipotent mesenchymal stem cells (MSCs) for organ regeneration, are being pursued for cardiac disease, orthopedic injuries and biomaterial fabrication. The molecular pathways that regulate MSC-mediated regeneration or enhance their therapeutic efficacy are, however, poorly understood. We compared MSCs isolated from MRL/MpJ mice, known to demonstrate enhanced regenerative capacity, to those from C57BL/6 (WT) mice. Compared with WT-MSCs, MRL-MSCs demonstrated increased proliferation, in vivo engraftment, experimental granulation tissue reconstitution, and tissue vascularity in a murine model of repair stimulation. The MRL-MSCs also reduced infarct size and improved function in a murine myocardial infarct model compared with WT-MSCs. Genomic and functional analysis indicated a downregulation of the canonical Wnt pathway in MRL-MSCs characterized by significant up-regulation of specific secreted frizzled-related proteins (sFRPs). Specific knockdown of sFRP2 by shRNA in MRL-MSCs decreased their proliferation and their engraftment in and the vascular density of MRL-MSC-generated experimental granulation tissue. These results led us to generate WT-MSCs overexpressing sFRP2 (sFRP2-MSCs) by retroviral transduction. sFRP2-MSCs maintained their ability for multilineage differentiation in vitro and, when implanted in vivo, recapitulated the MRL phenotype. Peri-infarct intramyocardial injection of sFRP2-MSCs resulted in enhanced engraftment, vascular density, reduced infarct size, and increased cardiac function after myocardial injury in mice. These findings implicate sFRP2 as a key molecule for the biogenesis of a superior regenerative phenotype in MSCs.

regeneration | wound healing

Bone marrow (BM)-derived MSCs can regenerate diseased myocardium and accelerate bone and soft tissue repair (1–3). MSCs are rare in the BM but can be isolated by selecting the adherent, spindle-shaped cells that expand from mononuclear cells in humans, rodents and pigs (4–6). Engrafted MSCs dramatically reduce the extent of necrotic myocardium and promote the regeneration of new, contractile myocardium (1, 7, 8). As with other BM-derived cells, the molecular pathways that modulate MSC-mediated tissue repair are not completely understood.

To better understand the role of stem cells in regenerative biology, we studied the "superhealer" MRL/MpJ mouse, generated by interbreeding 4 different strains (9). This strain was found to be capable of completely closing 2 mm surgical ear holes within 30 days whereas control (Bl/6) mice leave residual, open holes (10). Upon right ventricular cryoinjury, this "superhealer" demonstrated regeneration of the wound with scarless myocardium, whereas the control mice demonstrated acellular scars (11). Using a BM sex-mismatched transplant model, the authors showed that MRL hearts had 3-fold greater BM-derived cells in the myocardium than uninjured animals or injured WT mice (11). More recently, the group showed that myocardial regeneration in this model could be recapitulated in WT (C57BL/6) mice after BM engraftment with hematopoietic cells derived from MRL/MpJ fetal liver (12). This led us to hypothesize that BM-derived cells from the MRL strain may exhibit an enhanced regenerative phenotype. Our findings show enhanced efficacy of BM-derived MRL-MSCs and demonstrate that this phenotype is due to the activity of the Wnt signaling modulator, secreted frizzled-related protein 2 (sFRP2).

Wnt/β-catenin signaling is necessary for the commitment/differentiation of mesenchymal cells to osteocytes, chondrocytes and adipocytes (13–16). Consistent with this, the Wnt inhibitor, Dkk1, promotes human MSC self-renewal (17). sFRP family of proteins bind directly to Wnts to prevent receptor binding and activation of Wnt signaling (18). Our study shows that sFRP2 directly modulates MSC proliferation and engraftment and that increased sFRP2 expression in MSCs is associated with enhanced therapeutic efficacy of MSC therapy in wound granulation tissue formation and in repair of infarcted myocardium.

Results

Isolation and Characterization of 2 Populations of MSCs. Murine MSCs were isolated from both MRL/MpJ (MRL, $n = 2$ independent lines) and Bl/6 (WT) strain (an additional Bl/6 MSC isolate was purchased from Tulane Center for Gene Therapy). The MSCs were characterized by immunofluorescent staining and confirmed to be $CD45^-$, $CD11b^-$ (data not shown). These MSCs were positive for the cell surface antigens $Sca1^+$ and $CD44^+$ as analyzed by flow cytometry [supporting information (SI) Fig. S1*a*]. To confirm MSC phenotype (19, 20), each line was shown to be capable of differentiation along 3 principal lineages: osteoblast, adipocyte, and chondrocyte (Fig. S1 *b* and *c*). Studies were performed with at least 2 different MSC lines of each phenotype and the data combined.

MRL-MSCs Engrafted Extensively and Induced Vigorous, Well-Vascularized Granulation Tissue. To compare the effect of the different MSCs in promoting both the quantity and quality of granulation tissue deposition, we used the PVA sponge model of repair stimulation. This model is widely used to study granulation tissue deposition resembling healing by secondary intention (21, 22). MSC engraftment (persistence in tissue), vascularity, and organization of the resultant granulation tissue were compared among sponges implanted into the same animal and across multiple animals. When implanted into mice genetically deficient for β-glucuronidase (β-gluc), both WT- and MRL-loaded sponges gave rise to abundant

Author contributions: P.P.Y. designed research; M.P.A., M.P., A.V., M.F.H., and P.P.Y. performed research; E.L. contributed new reagents/analytic tools; M.P.A., J.A., J.C., J.M.D., J.R., E.L., and P.P.Y. analyzed data; and P.P.Y. wrote the paper.

The authors declare no conflict of interest.

This article is a PNAS Direct Submission.

[1]To whom correspondence should be addressed. E-mail: pampee.young@vanderbilt.edu.

This article contains supporting information online at www.pnas.org/cgi/content/full/0803437105/DCSupplemental.

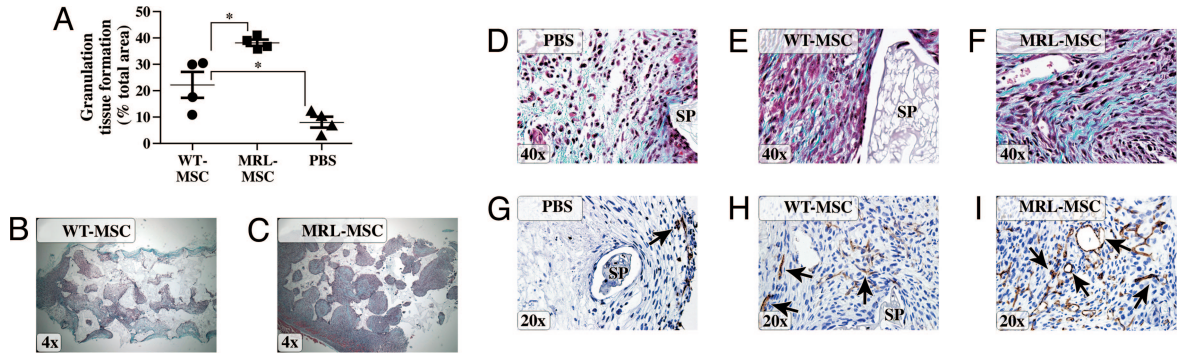

Fig. 1. MRL-MSCs generated more advanced wound granulation tissue. (*A*) Graph of granulation tissue area in representative histologic sponge sections as a percentage of total sponge area. One-way ANOVA with Bonferrroni correction was used to compare data between WT vs. MRL or PBS, $n = 4$ in each group. Representative low power Trichrome images show decreased granulation tissue in WT- (*B*) vs. MRL- (*C*) MSC-loaded sponges. (*D–F*) High power Trichrome images show that MSC-loaded sponges (*E* and *F*) were more organized, highly cellular and with abundant type I collagen (blue) as compared with PBS control (*D*). (*G–I*) Representative immunostained sections using anti-PECAM-1 to designate vascular density from PBS-loaded (*G*), WT (*H*), or MRL (*I*) MSC-derived sponge granulation tissue. SP, sponge matrix, arrows point at positive stain, *, $P < 0.05$.

granulation tissue compared with sponges loaded with vehicle (PBS) (Fig. 1 *A–C*). This enabled us to distinguish β-gluc-positive MSC-derived tissue (i.e., assess engraftment) from β-gluc-negative host tissue. Sponges injected with MRL-MSCs had significantly greater amount of granulation tissue over a given cross-sectional area than those loaded with WT-MSCs (Fig. 1 *A–C*). Granulation tissues observed in sponges treated with MRL-MSCs (Fig. 1 *C* and *F*) and WT-MSCs (Fig. 1 *B* and *E*) appeared highly organized with abundant collagen deposition. By contrast, sponges treated with PBS (Fig. 1*D*) demonstrated loose, disorganized tissue architecture with markedly reduced collagen deposition. The majority of the granulation tissue in MSC-loaded sponges (Fig. S1*d*) showed substantial engraftment with implanted MSCs as evidenced by the extensive, red (β-gluc-positive) histochemical staining whereas the PBS-loaded sponges (negative control) contained only β-gluc-negative host cells. Biochemical measurement for β-gluc enzyme activity (a quantitative measure of MSC engraftment) showed greater than 3-fold increased engraftment of MRL-MSCs compared with WT-MSCs (Fig. 2*A*). Furthermore, the granulation tissue derived from MRL-MSCs was comparatively more vascularized than that from WT-MSCs as determined by greater density of PECAM-1 immunopositive vascular structures (Figs. 1 *H* and *I* and 2*B*). The observed increased engraftment with MRL-MSCs is consistent (in part) with greater than 2-fold increased in vitro proliferation of MRL-MSCs over WT-MSCs (Fig. 2*C*). However, the number of cells (affected by proliferation rate) does not correlate directly with engraftment, suggesting that these are distinct mechanisms (23).

MRL-MSCs Displayed a Down-Regulation of Wnt Target Genes and Increased Expression of sFRPs. To determine the molecular basis for the enhanced repair properties of MRL-MSCs, we compared their gene expression to WT-MSCs. Several inhibitors of the β-catenin/Wnt (canonical) signaling pathway belonging to the sFRP family were significantly enriched in MRL-MSCs (Fig. 3*A*). An evaluation of target genes that are known to be transcriptionally up-regulated by the canonical Wnt pathway (and hence should be decreased in MRL-MSCs) uncovered 3 genes, Cyclin D1 (24), Sox2 (25) and Axin2 (26), that had >4-fold reduced expression in MRL-MSCs (Fig. 3*A* and Table S1). Interestingly, the microarray data showed increased Wnt4 transcripts in MRL-MSCs. Wnt4 is involved in regulating mesenchymal to epithelial transformation in the kidney and whose activity is thought to be regulated by sFRP2; in other reports Wnt4 induces sFRP2 expression (27). Quantitative real-time RT-PCR confirmed the gene expression differences for a subset of these genes (Table S1 and Table S2). sFRP2 and sFRP4 transcripts were up-regulated in MRL-MSCs by >250- and 30-fold, respectively. The aforementioned canonical target genes were significantly downregulated in MRL-MSCs between 5- and 12-fold, consistent with the genomic profile (Table S1).

This gene expression signature would predict a reduction in canonical Wnt signaling in MRL-MSCs. An optimized version of the TOPFlash reporter was used to compare constitutive β-catenin-mediated transcriptional activation in MRL- and WT-MSCs (28) (Fig. 2*D*). Consistent with our prediction, MRL-MSCs exhibited a significant reduction in TOPFlash/FOPFlash ratio under basal conditions. We next assessed if murine and human MSC proliferation was modulated by Wnt signaling (Fig. 3*B*). Wnt pathway activation through either addition of LiCl or recombinant murine Wnt3a decreased proliferation for both murine (WT and MRL) and human MSCs; the small decrease of human MSC proliferation with Wnt3a treatment was not statistically significant, possibly

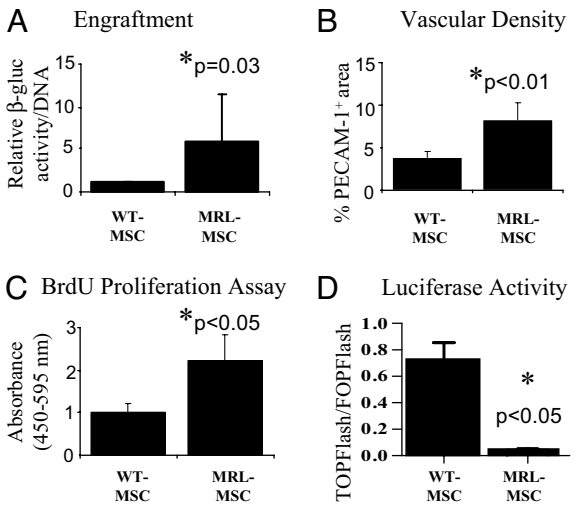

Fig. 2. MRL-MSCs showed higher engraftment, vascularity. (*A*) β-gluc-specific activity (MSC marker) normalized to total cellular DNA content of paired WT- and MRL-MSC sponge granulation tissue samples were calculated and the average of the fold change for $n = 7$ animals were graphed to represent engrafted MSCs. (*B*) Vascular density graphed as percentage of immunopositive PECAM-1 area/total tissue area in histologic sections from granulation tissue. Data represents averages of multiple 40X fields from unpaired samples ($n = 6$). (*C*) In vitro proliferation of WT- and MRL-MSCs using BrdU ELISA; $n = 5$ experiments performed in triplicate. (*D*) Basal normalized luciferase activity; $n = 2$ experiments performed in duplicate. Unpaired Student's *t* test was used.

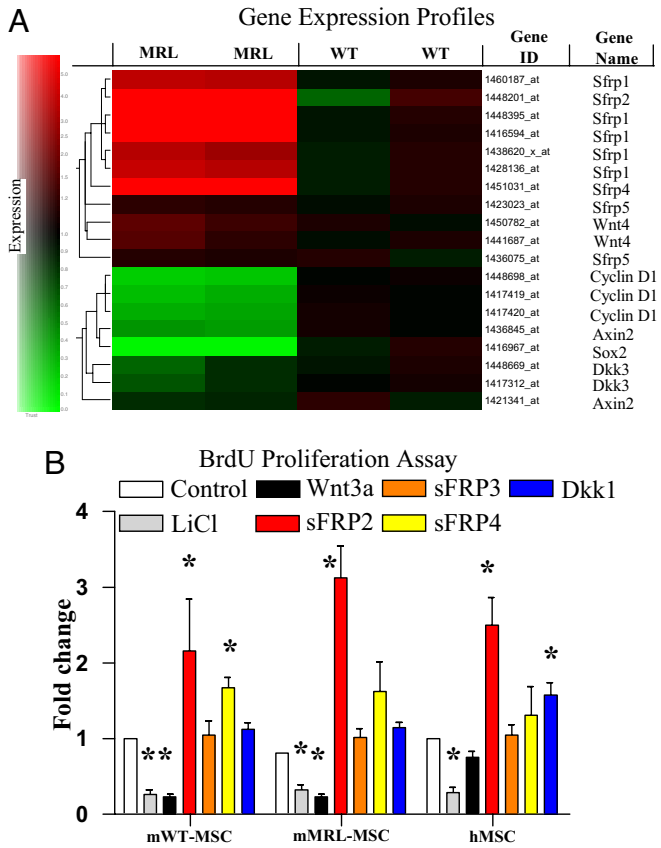

Fig. 3. MRL-MSCs demonstrated a downregulation of canonical Wnt pathway by up-regulation of sFRPs. (*A*) Expression of known Wnt pathway genes (rows) in MSCs isolated from WT and MRL mice in duplicate experiments, from low (green) to high (red). Gene tree (to the left of the rows) corresponds to the degree of similarity of the pattern of expression for genes. (*B*) In vitro proliferation of murine and human MSCs relative to basal levels (e.g., media alone) in the presence of LiCl (10 mM) or various recombinant Wnt pathway factors: 50 ng/ml Wnt3a, 100 ng/ml sFRP2, 100 ng/ml sFRP3, 2 μg/ml sFRP4, or 100 ng/ml Dkk1. The data shown are the fold change relative to media alone within each given cell type. Data are from at least 3 experiments performed in triplicate. Unpaired Student's *t* test with Bonferroni's correction was used. *, $P < 0.05$.

reflecting species-specific differences in Wnt/Frizzled receptors. Dkk1, surprisingly, did not affect murine MSCs but showed a statistically significant increase with human MSC proliferation in vitro, consistent with previous studies (17, 29). Although sFRP4 increased WT-MSC proliferation, only sFRP2 mediated a consistent and notable increase in proliferation in both murine and human MSC lines. To underscore the significance of the Wnt pathway in engraftment of MRL-MSCs in vivo, we injected LiCl every other day directly into WT- or MRL-MSC preloaded sponges. As anticipated, LiCl-mediated activation of canonical Wnt signaling significantly reduced MRL-MSC engraftment to levels comparable with WT-MSCs (Fig. S2).

MSCs Differentially Expressed Wnt Constituents. To investigate the contribution of secreted Wnt pathway members on the regulation of β-catenin in MSCs in vivo, we generated stably-transduced WT-MSC lines overexpressing Wnt3a, Dkk1 or sFRP2. Coexpression of GFP with each cDNA enabled FACS enrichment of vector-transduced MSCs (>90%; data not shown; see Table S3). Control transducts were generated that expressed GFP alone (GFP-MSC). Fold increase of sFRP2 protein expression in transduced WT cells (sFRP2-MSCs) assessed by immunoblot was comparable to the fold increase observed between GFP-MSCs and MRL-MSCs (Fig. 4*A*). Wnt3a expression was verified by immunofluorescent staining of sorted (GFP-positive) cells as it was difficult to obtain sufficient numbers of cells for an immunoblot (Fig. S3*a*); overexpression of Wnt3a in MSCs (Wnt3a-MSCs) abrogated their proliferation in culture (Fig. 4*B*). MSC transducts expressing Dkk1 (Dkk1-MSCs), sFRP2 or GFP retained the capacity for trilineage differentiation (Fig. S3 *b* and *c*) and express CD44 and Sca1 by FACS (data not shown). Regulation of canonical Wnt signaling activity of conditioned media from each MSC transduct line was assessed in HEK 293 cells stably transfected with TOPFlash Wnt reporter system. Recombinant protein was used as a positive control. As expected, conditioned media from Wnt3a-MSC resulted in increased luciferase activity over conditioned media from vector-transfected MSCs (GFP-MSC), whereas conditioned media from Dkk1- or sFRP2-MSCs resulted in comparatively reduced β-catenin-mediated transcriptional activity (Fig. S3*d*). Wnt signaling in sFRP2-MSCs was decreased compared with GFP-MSCs as assessed by luciferase activity after transfection with TOP/FOPFlash reporter constructs (Fig. S3*e*).

sFRP2 Enhanced MSC-Mediated Wound Repair. As discussed, Wnt3a expression abolished MSC proliferation and these cells died after 4–6 weeks in culture. By contrast, overexpression of sFRP2 resulted in >3-fold increase in proliferation as compared with GFP-MSC (Fig. 4*B*). Overexpression of Dkk1 did not alter the proliferation rate over GFP-MSCs (Fig. S4*b*). These effects are consistent with our observation using recombinant proteins (Fig. 3*B*). Moreover, further testing of Dkk1-MSC transducts failed to show changes in murine MSC engraftment or MSC-derived sponge granulation tissue (Fig. S4*c*) over GFP-MSCs, suggesting that murine MSCs, unlike human MSCs, failed to respond to Dkk1-mediated Wnt inhibition.

To assess the role of the Wnt inhibitor sFRP2 in promoting both the quantity and quality of MSC-generated granulation tissue, we loaded PVA sponges with sFRP2- or GFP-MSCs before implantation into β-gluc-deficient mice. β-gluc enzyme activity in granulation tissue was significantly increased (>3-fold) in sFRP2-MSC-loaded sponges compared with GFP-MSC-loaded controls (Fig. 4*C*). Furthermore, examination of vascular density using PECAM-1 immunostaining showed that granulation tissue generated from sFRP2-MSCs was more densely vascularized than GFP-MSCs (Fig. 4*D*). To examine if sFRP2-MSCs directly contributed to the microvasculature of granulation tissue, we performed colocalization by confocal microscopy using anti-GFP (to identify MSCs) and anti-PECAM-1. MSC-derived vascular structures were evident within the MSC-derived granulation tissue (Fig. S5*a*) suggesting that MSCs underwent transdifferentiaion into the endothelial lineage to contribute to repair tissue vasculature.

Proliferation and Enhanced Engraftment of MRL-MSCs Are Mediated by sFRP2. We sought to determine is sFRP2 inhibition could abrogate the MRL-MSC phenotype. Knockdown of sFRP2 mRNA transcripts with 3 independent shRNAs were assessed by real-time RT-PCR (Table S4). MRL-kd-MSCs (derived using shRNA clone 75B) were expanded and further tested by immunoblot and showed a ≈70% reduction in sFRP2 protein as compared with MRL-MSCs stably transduced with control shRNA (Fig. 4*A*). Specific sFRP2 knockdown also decreased proliferation by 2-fold over control shRNA-MSCs (Fig. 4*B*). Furthermore, MRL-kd-MSCs showed >5-fold decrease in MSC engraftment in experimental granulation tissue (Fig. 4*C*). Importantly, the experimental granulation tissue generated by MRL-kd-sFRP2 were also 3-fold less densely vascularized, as assessed by PECAM-1 staining, when compared with control shRNA MRL-MSCs-loaded sponges (Fig. 4*D*).

sFRP2 Facilitated MSC Engraftment and Cardiac Remodeling/Repair. We then assessed whether sFRP2 overexpression could improve MSC-mediated myocardial regeneration by injecting sFRP2-MSCs,

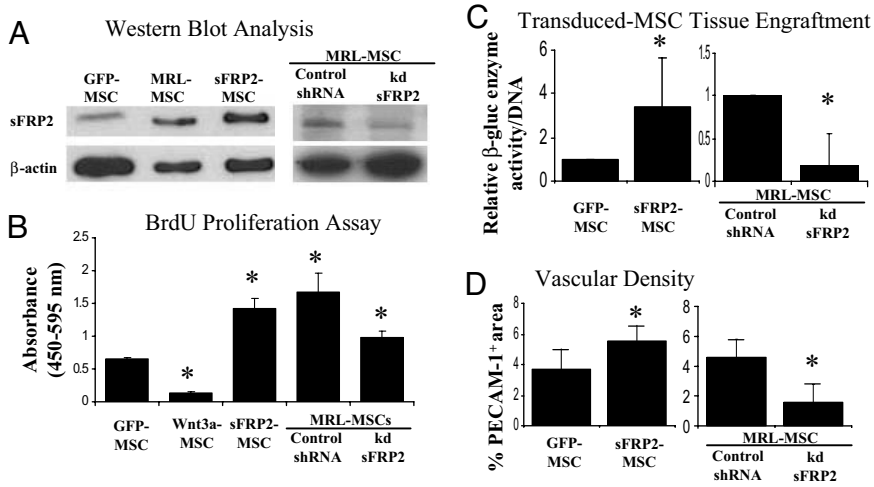

Fig. 4. sFRP2 promotes MSC proliferation, engraftment and vascular density of stem cell generated granulation tissue. (*A*) sFRP2-MSCs were sorted for GFP expression and analyzed by immunoblot for specific protein expression. WT-MSCs transduced with vector containing GFP alone (GFP-MSC) were also sorted in parallel. MRL-MSCs transduced with lentiviral control construct (Control shRNA) and MRL-MSCs with shRNA knockdown of sFRP2 (MRL-kd-sFRP2, clone 75B) were selected by puromycin resistance and analyzed by immunoblot for specific protein expression. (*B*) Cell proliferation assay of GFP-MSCs, MSCs expressing specific Wnt pathway components, Control shRNA, and MRL-kd-sFRP2 (clone 75B) $n \geq 3$ independent experiments. (*C*) β-gluc specific activity normalized to total cellular DNA content of paired GFP-MSCs and sFRP2-MSC loaded granulation tissue and MRL-kd-sFRP2 paired to Control shRNA loaded sponges. $n = 5$ sponges of each condition. (*D*) Vascular density of granulation tissue derived from sFRP2-MSCs compared with control MSCs and MRL-kd-sFRP2 MSCs compared with Control shRNA graphed as percentage of immunopositive PECAM-1 area/total tissue area in 40× fields. One-way ANOVA with Bonferrroni correction was used to compare the proliferation data. Paired Student's *t* test was used for comparisons of engraftment and vascularity data. *, $P \leq 0.05$.

GFP-MSCs, MRL-MSCs, or vehicle PBS into the periinfarct area of the left ventricle after coronary artery ligation. Ventricular remodeling and cardiac function were analyzed by echocardiography at 7 and 30 days post MI (Table 1). Left ventricle (LV) internal dimension diastolic (LVIDD) and LV internal dimension systolic (LVIDS) reflect remodeling of the infarcted ventricle. At 30 days post MI, both dimensional parameters were smaller in the MRL-MSC and sFRP2-MSC recipients, suggesting a role for sFRP2 in chamber remodeling. The percentage difference in LVIDS between day 7 and day 30 was significantly reduced in animals receiving sFRP2-MSCs (Fig. 5*A*). When compared with the GFP-MSC, recipients of both the MRL-MSC and sFRP2-MSC showed improved ventricular remodeling. To determine whether sFRP2 improved cardiac function, the percentage differences in ejection fraction (EF) and fractional shortening (FS) (Fig. 5*B*) between 7 and 30 days after treatment were analyzed (Table 1). The MRL recipients showed an increase in both ΔEF (2.17%) and ΔFS (3.18%) when compared with WT-MSC (−7.28% and −10.28%, respectively) and PBS-injected (−9.89% and −13.17%, respectively) controls. In contrast, sFRP2-MSC cohorts exhibited significant functional improvement 30 days post infarct (ΔEF 6.24% and ΔFS 13.82%). These results together indicate sFRP2 overexpression has a significant positive effect on cardiac function.

Mean percentage of LV area infarcted in PBS-treated control animals was 26 ± 10% (Fig. 5*C* and Fig. S5*b*). Injection of GFP-MSCs had a modest protective effect, limiting the extent of the infarction to 14% of LV (p = NS) (Fig. 5*C*). In contrast, injection of MRL-MSCs significantly limited infarct size to 6.0% of the LV ($P < 0.05$ vs. PBS). Notably, injection of sFRP2-MSCs limited infarct size even more dramatically to 3.4% ($P < 0.05$ vs. PBS and the GFP-MSC group). Compared with the PBS group, we observed a relative reduction in infarct size of 12% in the GFP-MSC group and 23% in the sFRP2-MSC group.

Myocardial engraftment of MSCs was assessed by counting GFP-positive cells. Whereas significant engraftment was evident grossly within granulation tissue of sponge implants (Fig. 1*G* and Fig. S5*c*), the numbers of MSCs within the myocardium 30 days after injection were comparatively fewer (Fig. S5*c*). However, the sFRP2-MSCs resulted in a significant increase in the number of engrafted MSCs compared with controls (Fig. 5*D*). We examined the myocardial scar region for colocalization of GFP-MSCs with endothelial (anti-PECAM-1) or cardiomyocyte (anti-α-actinin) specific marker and did not observe any (data not shown). Vascular density of the scarred region was assessed by immunohistochemistry for PECAM-1 and showed a statistically significant increase with sFRP2-MSCs compared with GFP-MSCs (Fig. 5*E* and Fig. S5*d*).

Discussion

Although MSCs are a promising source of cell therapy for heart and wound regeneration, little is known about the molecular pathways that modulate MSC-mediated regeneration and repair (3, 23). Furthermore, the extent to which repair and regeneration mediated by MSCs relies on their engraftment and direct contribution versus serving as effectors to alter the stem cell microenvironment is not understood (3). The distinct soft tissue repair models used in this

Table 1. sFRP2 aids in remodeling and improves function of injured hearts

	PBS		GFP-MSCs		MRL-MSCs		sFRP2-MSCs	
	d7	d30	d7	d30	d7	d30	d7	d30
LVIDD, cm	0.31 ± 0.05	0.36 ± 0.06	0.34 ± 0.07	0.37 ± 0.08	0.28 ± 0.02	0.26 ± 0.03	0.32 ± 0.03	0.34 ± 0.04
LVIDS, cm	0.19 ± 0.04	0.21 ± 0.04	0.20 ± 0.08	0.25 ± 0.08	0.16 ± 0.01	0.13 ± 0.03	0.18 ± 0.04	0.17 ± 0.03
FS	39.7 ± 5.68	34.3 ± 7.70	36.7 ± 8.8	32.7 ± 10.1	43.92 ± 5.21	45.74 ± 7.27	43.5 ± 7.41	48.6 ± 4.50
EF	0.77 ± 0.05	0.69 ± 0.10	0.72 ± 0.12	0.67 ± 0.13	0.81 ± 0.06	0.83 ± 0.07	0.80 ± 0.08	0.85 ± 0.04
ΔLVIDS, %	19.98 ± 28.38§		30.36 ± 30.13†‡		−18.28 ± 19.80‡§		−5.07 ± 14.53†	
ΔFS, %	−13.17 ± 15.71*		−10.28 ± 16.33†		3.81 ± 6.79		13.82 ± 16.17*†	
ΔEF, %	−9.89 ± 12.39*		−7.28 ± 10.68†		2.17 ± 2.21		6.24 ± 7.33*†	

The top four rows represent the mean and standard error mean (± SEM) values for each treatment at day 7 and day 30. The mean ± SEM percentage difference (Δ%) values are in the bottom three rows. One-way ANOVA with Newman–Keuls multiple comparison test was used to compare the Δ% values for each echocardiographic parameter. *, $P < 0.05$ PBS vs. sFRP2-MSC; †, $P < 0.05$ GFP-MSC vs. sFRP2-MSC; ‡, $P < 0.05$ GFP-MSC vs. MRL-MSC; §, $P < 0.05$ PBS vs. MRL-MSC. PBS $n = 7$, GFP-MSC $n = 6$, MRL-MSC $n = 5$, sFRP2-MSC $n = 7$.

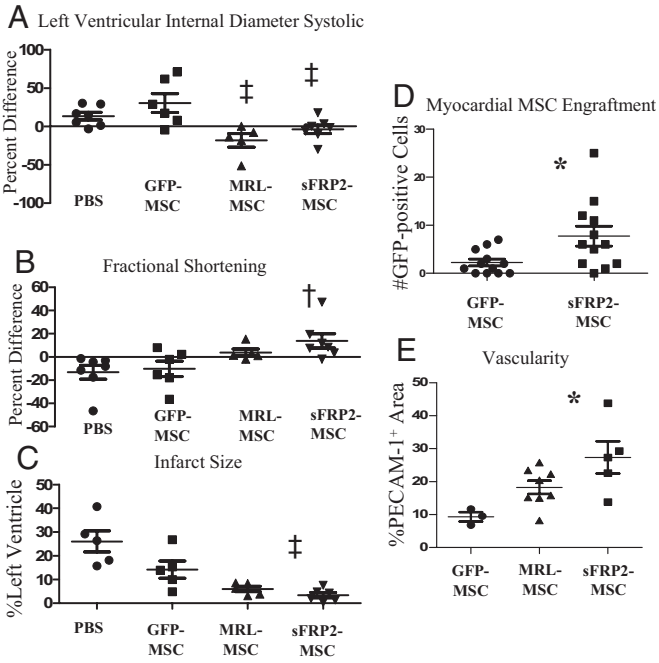

Fig. 5. sFRP2 aids in remodeling and improves function of injured hearts. Fractional shortening (*A*) and LVIDS (*B*) determined by echocardiography are plotted as percentage difference (Δ%) values (mean +/- SEM) between 7 and 30 days after infarct to reflect therapy-mediated impact on remodeling or function. Increased Δ% in FS measured in sFRP2-MSC-treated hearts compared with GFP-MSC-treated hearts demonstrates enhanced cardiac function. (*C*) Infarct size was significantly attenuated in hearts injected with sFRP2-MSCs compared with control GFP-MSCs. One-way ANOVA and Newman–Keuls multiple comparison test: $^{\dagger}P < 0.05$ vs. PBS and GFP-MSC; $^{\ddagger}P < 0.05$ vs. GFP-MSC. (*D*) Engraftment of transplanted MSCs within myocardial sections 30 days after MI, immunohistochemistry for GFP. (*E*) PECAM-1-positive structures reflecting microvessel density within scar tissue were quantified. *, $P < 0.05$ using One-way ANOVA with Newman–Keuls post test. (Representative photomicrographs of infarct histology are shown in Fig. S5*c*.)

study provided different in vivo contexts to study MSC-driven therapy. The sponge soft tissue repair model also permitted clear demarcation and evaluation of angiogenesis, organization, and contribution of MSC-derived granulation tissue. The isolation and characterization of 2 strain specific populations of MSCs with differing in vivo regenerative properties led us to identify sFRP2 as a key molecule that mediates self-propagation of both human and mouse MSCs in vitro and whose overexpression enhanced MSC-mediated angiogenesis and therapeutic potency.

A role for Wnt signaling in modulating MSC biology was suggested by molecular profiling of the MSC populations isolated from the regenerative MRL/MpJ mice, as compared with the MSCs isolated from WT (Bl/6) strain. Together, our data suggest that Wnt signaling inhibition correlated with the superior properties exhibited by MRL-MSCs; these included enhanced proliferation and the ability to mediate more abundant, better organized and vascularized granulation tissue in implanted PVA sponges. Consistent with our findings, several lines of evidence from published reports (13–16) support a role for Wnt inhibition in regulating mesenchymal stem cell self-renewal and expansion. Importantly, Wnt/β-catenin activation has been shown to be necessary for the commitment/differentiation of mesenchymal cells to osteocytes, chondrocytes, myoblasts, and adipocytes (13–16). Additionally, Dkk1, an inhibitor of the canonical Wnt pathway, increased human MSC proliferation and promoted entry into the cell cycle in vitro (17). Consistent with these studies, our findings support a role for canonical Wnt activation in MSC lineage commitment and, conversely, Wnt inhibition in self-renewal.

Recently, Liu *et al.* (30) reported that accelerated aging and associated depletion and dysfunction in stem cells in various tissues and organs is associated with increased Wnt activity. Expression of klotho, a secreted protein that binds and sequesters Wnt and leads to suppression of Wnt activity, and its absence in mice leads to early onset age-related changes (30). Another study found that activation of Wnt signaling promoted tissue specific stem cell aging and increased tissue fibrosis (31). Both studies broadly support our hypothesis and link Wnt inhibition to stem cell maintenance and function (30, 31).

We identified an effect of sFRP2, an inhibitor of Wnt signaling, on MSC self-propagation by comparing MSCs from mouse strains with markedly different healing properties. Whereas canonical Wnt activation, either through addition of exogenous activators or by induced overexpression of Wnt3a, dramatically inhibited baseline MSC proliferation, addition of sFRP2 resulted in significantly increased proliferation of both mouse and human MSCs. This increase was much greater than that seen with other sFRPs tested and recombinant Dkk1, which caused a statistically significant increase in hMSC proliferation. Dkk1 inhibits Wnt signaling by binding to LRP5 and LRP6 and blocking their interaction with Wnt and Frizzled (32). Kremen 1 and 2 are transmembrane Dkk1 receptors that synergize with Dkk1 to inhibit Wnt signaling (32). Kremen transcripts were undetected in murine MSCs through microarray analysis (data not shown). This observation may explain the lack of response of murine, but not human, MSCs to Dkk1. Interestingly, despite the very high level of endogenous sFRP2 in MRL-MSCs, addition of increasing amounts of recombinant sFRP2 continued to increase proliferation, suggesting significant residual Wnt activity and/or non-canonical roles of sFRP2. Moreover, specific knockdown of sFRP2 in MRL-MSCs resulted in abrogation of the comparatively enhanced wound tissue reconstitution phenotype observed in MRL-MSCs.

MSCs genetically modified to overexpress sFRP2 or Dkk1 were used to investigate the effect of these factors in MSC-mediated tissue repair. Importantly, increased constitutive expression of either Wnt pathway molecule did not abolish expression of mouse MSC surface markers, such as CD44 or Sca1, or the capacity for multilineage differentiation, albeit our experiments did not address whether these factors affected differentiation kinetics. sFRP2-MSCs replicated the MRL-MSC phenotype of enhanced engraftment in situ, increased angiogenesis, and in the setting of acute myocardial injury, resulted in significantly reduced infarct size. Consistent with the histological data, there was enhanced residual myocardial function and attenuation of adverse cardiac remodeling 30 days post MI. Although the numbers of sFRP2-MSCs remaining 30 days post infarction (engraftment) were greater than GFP-MSCs, the overall number of implanted MSCs remaining in the myocardium was considerably lower than those comprising the granulation tissue formed in the sponge model (Fig. S5). This finding would suggest that type of injury and the stem cell microenvironment may influence the underlying mechanisms of repair, i.e., direct contribution vs. paracrine effects. The data also suggest that the injury environment may dramatically affect implanted stem cell survival and persistence in vivo. The molecular signals that impact the degree of MSC engraftment are not known.

sFRP2 was first isolated from a BM-derived stromal cell line and was proposed to serve as an inhibitor of Wnt signaling by binding and sequestering the *Drosophila* Wnt homologue, Wingless (33). Subsequent studies have shown inhibition of Wnt signaling by direct binding to and sequestering of Wnt3a (34). sFRP2 has been shown to protect against UV- or TNF-induced apoptosis in a canine cancer cell line (18). Recently sFRP2 was found to be a key factor secreted by genetically engineered MSCs overexpressing Akt (35). This last study showed that much of the MSC-mediated improvement in myocardial function resulting from Akt-MSC therapy could be attributed to a downstream increase in sFRP2. Moreover, sFRP2 was shown to directly prevent cardiomyocyte death, and thereby,

serve as a stem cell-derived paracrine factor to influence cardiomyocyte survival and repair (35). The enhanced myocardial repair observed in our study can be attributed, at least in part, to this mechanism. Our study also demonstrated that sFRP2 caused a robust increase in MSC therapy-induced angiogenesis. sFRP1 and 4 overexpression in endothelium have recently been shown to increase neovascularization in hindlimb ischemia by regulation of Wnt and Rac1 signaling (36). We do not know, however, whether sFRP2 works in a similar manner via direct paracrine effects on endothelial cells, indirectly via up-regulation of other angiogenic factors, or via MSC propagation. Notably, a variety of key proangiogenic genes are up-regulated in sFRP2-MSCs compared with GFP-MSCs as determined by gene expression profiling (Table S5). Finally, our findings also demonstrate that, in addition to potential paracrine function on target tissues, sFRP2 serves an autocrine and/or cell-intrinsic role in MSCs to mediate self-propagation and engraftment. MSCs appear to be multipotential effector cells whose own preservation and growth in vivo, such as those mediated by sFRP2, may lead to enhanced regenerative efficacy.

The mechanism by which sFRP2 modulates MSC proliferation and tissue engraftment is not known. sFRP2, but not other sFRPs tested, uniquely enhanced robust proliferation. Understanding the molecular regulation of MSCs by sFRP2 would have important implications for improving cell-based therapies using MSCs for wound and myocardial repair.

Materials and Methods

Materials. Lists of the antibodies, recombinant proteins, and cDNA clones are in *SI Materials and Methods*.

Animals/Surgical Interventions. All procedures were carried out in accordance with Vanderbilt Institutional Animal Care and Use Committee. Strains: C57Bl6 and NOD/SCID/β-glucuronidase-deficient (β-gluc$^{-/-}$) maintained by PPY; MRL/MPJ (The Jackson Laboratory). For repair/granulation tissue stimulation model, polyvinyl alcohol (PVA) sponge discs (4 mg, 2 mm height, 4 mm diameter) preloaded with MSCs (2.5×10^5 cells per sponge in 50 μL) or PBS and then implanted s.c. in adult mice. For MI model, anesthetized NOD/SCID (β-gluc WT) mice were intubated. A 7–0 silk suture was placed through the myocardium into anterolateral LV wall, ligating the left anterior descending artery. 2.5×10^5 WT ($n = 6$), MRL ($n = 5$), GFP ($n = 3$), or sFRP2 ($n = 8$) MSCs in 15 μL of PBS were injected into the peri-infarct area. The analyses of these interventions are detailed in *SI Materials and Methods*.

Cells. BM were collected from femurs of C57Bl6 mice and MRL/MPJ mice and MSCs generated as described in ref. 20. Detailed description of the isolation, characterization, differentiation and manipulation of these can be found in *SI Materials and Methods*.

RNA Isolation/Microarray. Details about RNA isolation, Affymetrix One Cycle reaction, hybridization to Mouse 430 2.0 array and analysis of the data can be found in *SI Materials and Methods*.

shRNA Knockdown of sFRP2. Detailed procedures for using Mission Lentiviral Transduction Particles (Sigma; catalog no. SRVRS) and appropriate control (Sigma #SHC002V) can be found in *SI Materials and Methods*.

Additional Methods. Methods for real-time RT PCR, transduction, immunoblot, histochemistry and morphometry, canonical Wnt signaling luciferase reporter, and statistical analyses are provided in *SI Materials and Methods*.

ACKNOWLEDGMENTS. This work was supported National Institutes of Health Grant HL088424, Veterans Affairs ARCD award, American Heart Association and Vanderbilt Discovery Award to PPY. All microarray experiments were performed in the Vanderbilt Microarray Shared Resource. Some of the materials used were provided by the Tulane Center for Gene Therapy through National Institutes of Health National Center for Research Resources Grant P40RR017447. Echocardiography and MI surgery were performed in the Cardiovascular Pathophysiology and Complications Core (CPCC) of the Vanderbilt Mouse Metabolic Phenotyping Center (MMPC), which is supported by the National Institute of Diabetes and Digestive and Kidney Diseases Grant U24 DK-59637.

1. Kinnaird T, *et al.* (2004) Local delivery of marrow-derived stromal cells augments collateral perfusion through paracrine mechanisms. *Circ* 109:1543–1549.
2. Falanga V, *et al.* (2007) Autologous BM-derived cultured MSCs delivered in a fibrin spray accelerate healing in murine and human cutaneous wounds. *Tissue Eng* 13:1299–1312.
3. Phinney DG, Prockop DJ (2007) Concise review: Mesenchymal stem/multipotent stromal cells: The state of transdifferentiation and models of tissue repair-current views. *Stem Cells* 25:2896–2902.
4. Colter DC, Sekiya I, Prockop DJ (2001) Identification of a subpopulation of rapidly self-renewing and multipotential adult stem cells in colonies of human marrow stromal cells. *Proc Natl Acad Sci USA* 98:7841–7845.
5. Jiang Y, *et al.* (2002) Pluripotency of MSCs derived from adult marrow. *Nature* 418:41–49.
6. Zimmet JM, Hare JM (2005) Emerging role for BM derived MSCs in myocardial regenerative therapy. *Basic Res Cardiol* 100:471–481.
7. Amado LC, *et al.* (2005) Cardiac repair with intramyocardial injection of allogeneic MSCs after myocardial infarction. *Proc Natl Acad Sci USA* 102:11474–11479.
8. Toma C, Pittenger MF, Cahill KS, Byrne BJ, Kessler PD (2002) Human MSCs differentiate to a cardiomyocyte phenotype in the adult murine heart. *Circ* 105:93–98.
9. McBrearty BA, Clark LD, Zhang XM, Blankenhom EP, Heber-Katz E (1998) Genetic analysis of a mammalian wound-healing trait. *Proc Natl Acad Sci USA* 95:11792–11797.
10. Heber-Katz E (1999) The regenerating mouse ear. *Semin Cell* Dev Biol 10:415–419.
11. Heber-Katz E, Leferovich JM, Bedelbaeva K, Gourevitch D, Clark LD (2004) The scarless heart and the MRL mouse. *Phil Trans R Soc Lond* 359:785–793.
12. Bedelbaeva K, *et al.* (2004) The MRL mouse heart healing response shows donor dominance in allogeneic fetal liver chimeric mice. *Cloning Stem Cells* 6:352–363.
13. Otto TC, Lane MD (2005) Adipose development: From stem cell to adipocyte. *Crit Rev Biochem Mol Biol* 40:229–242.
14. Gaur T, *et al.* (2005) Canonical Wnt signaling promotes osteogenesis by directly stimulating Runx2 gene expression. *J Biol Chem* 280:33132–33140.
15. Luo Q, *et al.* (2004) Connective tissue growth factor (CTGF) is regulated by Wnt and bone morphogenetic proteins signaling in osteoblast differentiation of MSCs. *J Biol Chem* 279:55958–55968.
16. Yano F, *et al.* (2005) The canonical Wnt signaling pathway promotes chondrocyte differentiation in a sox9-dependent manner. *Biochem Biophys Res Commun* 12:1300–1308.
17. Gregory CA, *et al.* (2005) Dkk-1-derived synthetic peptides and lithium chloride for the control and recovery of adult stem cells from BM. *J Biol Chem* 280:33132–33140.
18. Kawano Y, Kypta R (2003) Secreted antagonists of the Wnt signaling pathway. *J Cell Sci* 116:2627–2634.
19. Badoo M, *et al.* (2003) Characterization of MSCs isolated from murine BM by negative selection. *J cell Biochem* 89:1235–1249.
20. Tropel P, *et al.* (2004) Isolation and characterization of MSCs from adult mouse BM. *Exp cell Res* 295:395–406.
21. Krummel TM, *et al.* (1988) Transforming growth factor beta (TGF-beta) induces fibrosis in a fetal wound model. *J Pediatr Surg* 23:647–652.
22. Cooney R, Iocono J, Maish G, Smith JS, Ehrlich P (1997) Tumor necrosis factor mediates impaired wound healing in chronic abdominal sepsis. *J Trauma* 42:415–420.
23. Pittenger MF, Martin BJ (2004) MSCs and their potential as cardiac therapeutics. *Circ Res* 95:9–20.
24. Shtutman M, *et al.* (1999) The cyclin D1 gene is a target of the beta-catenin/LEF-1 pathway. *Proc Natl Acad Sci USA* 11:5522–5527.
25. Van Raay TJ, *et al.* (2005) Frizzled 5 signaling governs the neural potential of progenitors in the developing Exodus retina. *Neuron* 46:23–36.
26. Jho EH, *et al.* (2002) Wnt/beta-catenin/Tcf signaling induces the transcription of Axin2, a negative regulator of the signaling pathway. *Mol Cell Biol* 22:1172–1183.
27. Lescher B, Haenig B, Kispert A (1998) sFRP-2 is a target of the Wnt-4 signaling pathway in the developing metanephric kidney. *Dev Dyn* 213:440–451.
28. Veeman MT, Slusarski DC, Kaykas A, Louie SH, Moon RT (2003) Zebrafish prickle, a modulator of noncanonical Wnt/Fz signaling, regulates gastrulation movements. *Curr Biol* 13:680–685.
29. Gregory CA, Harpreet S, Perry AS, Prockop DJ (2003) The Wnt signaling inhibitor Dickkopf-1 is required for reentry into the cell cycle of human adult stem cells from BM. *J Biol Chem* 278:28067–28078.
30. Liu H, *et al.* (2007) Augmented Wnt signaling in a mammalian model of accelerated aging. *Science* 317:803–806.
31. Brack AS, *et al.* (2007) Increased Wnt signaling during aging alters muscle stem cell fate and increased fibrosis. *Science* 317:807–810.
32. Cselenyi CS, Lee E (2008) Context-dependent activation or inhibition of Wnt-b-catenin signaling by Kremen. *Science Signaling*, in press.
33. Rattner A, *et al.* (1997) A family of secreted proteins contains homology to the cysteine-rich ligand-binding domain of frizzled receptors. *Proc Natl Acad Sci USA* 94:2859–2863.
34. Wawrzak D, *et al.* (2007) Wnt3a binds to several sFRPs in the nanomolar range. *Biochem Biophys Res Commun* 357:1119–1123.
35. Mirotsou M, *et al.* (2007) Secreted frizzled related protein 2 (sFRP2) is the key Akt-mesenchymal stem cell-released paracrine factor mediating myocardial survival and repair. *Proc Natl Acad Sci USA* 104:1643–1648.
36. Dufourcq P, *et al.* (2007) Regulation of endothelial cell cytoskeletal reorganization by a secreted frizzled-related protein-1 and frizzled 4 and frizzled 7-dependent pathway: Role in neovessel formation. *Am J Pathol* 172:37–49.